Nano Res (2008) 1: 242–248
DOI 10.1007/s12274-008-8028-1
Research Article

Porous $LiFePO_4$/NiP Composite Nanospheres as the Cathode Materials in Rechargeable Lithium–Ion Batteries

Chunsheng Li, Shaoyan Zhang, Fangyi Cheng, Weiqiang Ji, and Jun Chen (✉)

Institute of New Energy Material Chemistry, Key Laboratory of Energy Material Chemistry (Tianjin) and Engineering Research Center of High-Energy Storage and Conversion (Ministry of Education), Nankai University, Tianjin 300071, China

Received: 5 May 2008 / Revised: 31 July 2008 / Accepted: 31 July 2008

ABSTRACT

We report the synthesis of porous $LiFePO_4$/NiP composite nanospheres and their application in rechargeable lithium-ion batteries. A simple one-step spraying technique was developed to prepare $LiFePO_4$/NiP composite nanospheres with an electrical conductivity 10^3–10^4 times that of bulk particles of $LiFePO_4$. Electrochemical measurements show that $LiFePO_4$ nanospheres with a uniform loading of 0.86 wt%–1.50 wt% NiP exhibit high discharge capacity, good cycling reversibility, and low apparent activation energies. The superior electrode performance of the as-prepared composite nanospheres results from the greatly enhanced electrical conductivity and porous structure of the materials.

KEYWORDS

Nanospheres, $LiFePO_4$/NiP, spraying, electrical conductivity, rechargeable lithium-ion batteries

Introduction

Developing new advanced materials is the most critical challenge in the fields of energy storage and energy conversion with high efficiency [1–4]. As an example, $LiFePO_4$ with the olivine structure has attracted great interest as the cathode material in rechargeable lithium-ion batteries because of its high-energy density, low cost, and safety [5–10]. However, the poor intrinsic electrical conductivity and the critical requirements of the synthesis procedures limit the large scale application of $LiFePO_4$. Various methods such as adding conductive carbon [11, 12], coating with a π-bonded polymer [13], reducing particle size [14], and doping with supervalent cations [15] have been employed in order to improve the electrical conductivity of $LiFePO_4$. It has also been found that a nano-network of conductive iron phosphide (Fe_2P) in the grain boundaries of $LiFePO_4$ can enhance its electronic conductivity [16]. Synthesis routes based on both solid phase and wet chemistry reactions have been used to prepare $LiFePO_4$ [17–19]. Generally, the as-prepared $LiFePO_4$ powders show irregular particle morphology with a broad particle size distribution, which results in low tapping density and energy density.

Herein, we report the incorporation of a nickel phosphorus alloy (NiP) in porous $LiFePO_4$/NiP composite nanospheres through a facile spraying technique. The method allows low reaction temperature and easy control over the preparation process, and hence can produce $LiFePO_4$/NiP composite nanospheres in high yield as well as with low cost and low energy consumption. Electrochemical

Address correspondence to chenabc@nankai.edu.cn

tests show that the as-prepared $LiFePO_4$ nanospheres with the addition of 0.86 wt%–1.50 wt% NiP are promising candidates as the cathode material of rechargeable lithium-ion batteries.

1. Experimental

1.1 Sample preparation

$LiFePO_4$/NiP composite nanospheres were prepared through a spraying technique with a modified Yamato Pulvis minispray instrument (Model GA-32) at a relatively low temperature of 350 °C (Electronic Supplementary Material (ESM), Fig. S-1) [20, 21]. The apparatus is divided into three parts comprising the droplet generator, pyrolysis reactor, and product collector. The pressure and temperature of the reaction system can be controlled. The pyrolysis reactor is a sloping chamber with an angle of about 45°, which can prolong the period of heating favoring the formation of fine particles. All the chemicals were of analytical grade and used as received without further purification. In a typical synthesis, 0.1 mol/L $Fe(NO_3)_3 \cdot 9H_2O$ and 0.1 mol/L LiH_2PO_4 were mixed and then a solution containing 5 mmol/L $NiSO_4 \cdot 6H_2O$, 6 mmol/L sodium citrate ($Na_3C_6H_5O_7 \cdot 2H_2O$), and 5 mmol/L $NaH_2PO_2 \cdot H_2O$ was added. The mixed solution was drawn into the apparatus by the fluid pump and transported to the outlet of the spray nozzle by pressurized high purity N_2 (99.999%, Air Products & Chemical Co. Ltd.) which also serves to control the system temperature. The sprayed droplets were heated at about 350 °C under the protection of N_2 gas during their descent of the pyrolysis reactor. The resulting particles were collected, washed with deionized water and ethanol, and then vacuum-dried at 80 °C for 4 h. By following the above procedures and changing the molar ratio of Fe to Ni, we obtained a series of $LiFePO_4$ nanospheres that contained 0, 0.35 wt%, 0.86 wt%, and 1.50 wt% NiP, as measured by inductively coupled plasma spectroscopy [22]. For comparison, $LiFePO_4$ bulk particles were prepared through a conventional solid-phase reaction [23] using Li_2CO_3, $NH_4H_2PO_4$, and $Fe(CH_3CO_2)_2$.

1.2 Characterization

Phase structures of the as-prepared samples were characterized using a Rigaku INT-2000 X-ray powder diffractometer (XRD) with Cu Kα radiation. The structural refinement for $LiFePO_4$ was performed with the RIETAN-2000 program [24]. Transmission electron microscopy (TEM) and high-resolution TEM (HRTEM) images were taken on a Philips Tecnai-F20 transmission electron microscope equipped with an energy dispersive X-ray (EDX) spectrometer. The tapping density of the samples was measured by tapping the powder 20 times in a 10 mL cylinder. Resistivity measurements were performed at room temperature using a four-point contact arrangement on a powered pellet (ø 8 mm × 10 mm). The specific surface areas of the products were measured by the Brunauer–Emmett–Teller (BET) method (Micromeritics ASAP 2010). Elemental analysis was carried out using a Hitachi P-5200 inductively coupled plasma spectrometer.

1.3 Electrochemical measurement

Electrochemical measurements were carried out using two-electrode cells with lithium metal as the counter electrode and reference electrode. The working electrodes were fabricated by compressing a mixture of 85 wt% active materials, 10 wt% acetylene black, and 5 wt% polytetrafluoroethylene onto an Al foil. The cell assembly was operated in a glovebox (Mikrouna China Universal 2240/750) filled with high purity argon (99.999%, Air Products & Chemical Co. Ltd.). The electrolyte was 1 mol/L $LiPF_6$ dissolved in a mixture of ethylene carbonate (EC) and diethyl carbonate (DEC) with the volume ratio of EC:DEC=1:1. Electrochemical performance was investigated using a Parstat 2273 potentiostat/galvanostat analyzer (Princeton Applied Research & AMETEK Company) and a modified Arbin charge-discharge unit at controlled temperatures [25, 26]. Cyclic voltammograms (CVs) were carried out at a scan rate of 1 mV/s and a temperature of 20 °C. Electrochemical impedance spectroscopy (EIS) was investigated at a voltage of 3.30 V in the frequency range $0.1–1\times10^6$ Hz. The electrode capacity was measured by a galvanostatic charge-discharge method at a constant current density of 50 mA/g to a cut-off voltage of 2.5 V at 20 °C. Charge-discharge cycles were tested with a current density of 50 mA/g

in the potential range 2.5–4.3 V. The capacity was calculated based on the amount of the active material, excluding the mass of the additives in the electrode.

2. Results and discussion

2.1 Characterization of the as-synthesized product

Figure 1(a) shows the XRD pattern and Rietveld analysis of the $LiFePO_4$ nanospheres containing 0.86 wt% NiP, while Fig. S-2 (in the ESM) displays the XRD patterns of the as-prepared $LiFePO_4$ bulk particles and nanospheres with different NiP contents. The diffraction peaks can be readily indexed to an orthorhombic phase with Pmnb space group (JCPDS-ICDD card No. 40-1499). No impurity peaks were observed. The cell parameters obtained from the Rietveld refinement are consistent with the standard value (Table S-1 in the ESM), indicating that addition

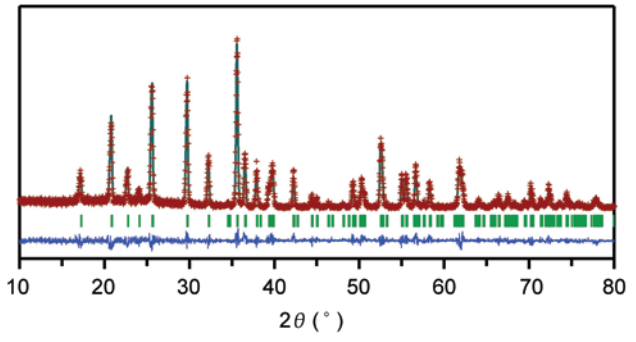

(a)

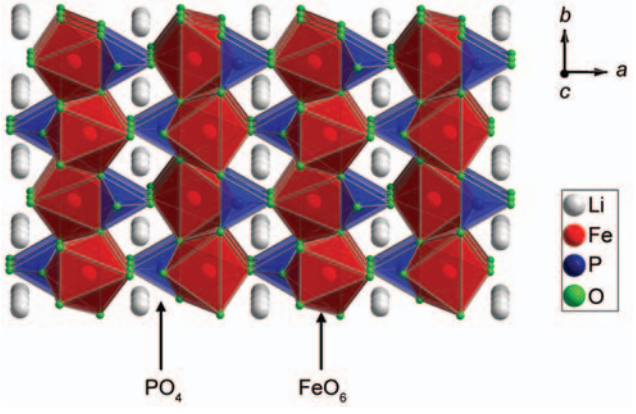

(b)

Figure 1 (a) Rietveld refinement of the XRD pattern of $LiFePO_4$ containing 0.86 wt% NiP. Red cross: observed intensity; green line: calculated intensity; blue solid line: the difference between the observed intensity and the calculated intensity; short green vertical bars indicate the positions of all possible reflections. (b) The crystal structure of $LiFePO_4$ viewed along the *c* axis

of a small amount of amorphous NiP does not have an effect on the crystal structure of $LiFePO_4$. Figure 1(b) shows the olivine structure of $LiFePO_4$, in which the dark-red octahedra represent Fe(II) coordinated by six oxygen atoms and the blue tetrahedra represent P(V) coordinated by four oxygen atoms. The Fe–O octahedra share corners with neighboring octahedra, forming a mesh layer which alternates with a layer of lithium chains. A P–O tetrahedron shares corners with its neighboring octahedra, embedded in the trough of the corrugated Fe–O layer. The structural characteristics facilitate the insertion/extraction of lithium ions.

Figure 2 shows representative TEM images of the as-prepared $LiFePO_4$ bulk particles and nanospheres. As shown in Fig. 2(a), the sample prepared by the conventional solid phase reaction route is composed of irregular shaped particles with sizes of up to micrometers. The as-synthesized $LiFePO_4$ nanospheres without any NiP (Fig. 2(b)) and with the addition of different amounts of NiP (Figs. 2(c)–(e)) consist mainly of nanospheres with an average diameter of about 200 nm. The proportion of the material with a nanosphere morphology in the $LiFePO_4$ nanospheres with the addition of 0.35 wt% and 0.86 wt% NiP is higher than that in $LiFePO_4$ nanospheres without NiP or with 1.5 wt% NiP. The HRTEM image (Fig. 2(f)) of one of the nanospheres in Fig. 2(d) shows the presence of a porous network structure with some disorder. Figures 2(g) and (h) show the elemental mapping of Ni and P in the $LiFePO_4$/NiP composite nanospheres, revealing that Ni and P are distributed homogeneously and the atomic ratio of Ni/P is close to 1:1.

The specific surface areas of the as-prepared $LiFePO_4$ bulk particles, nanospheres without NiP, and nanospheres containing 0.35 wt%, 0.86 wt%, and 1.5 wt% NiP are 6.2, 11.7, 15.8, 19.2, and 18.5 m^2/g, respectively. The tapping densities of the $LiFePO_4$ irregular particles and nanospheres are in the range 1.6–1.8 g/cm^3. The electrical conductivities of the as-prepared $LiFePO_4$ bulk particles, nanospheres without NiP, and nanospheres containing 0.35 wt%, 0.86 wt%, and 1.5 wt% NiP are 8.9×10^{-9}, 7.2×10^{-8}, 1.2×10^{-5}, 5.7×10^{-5}, and 1.2×10^{-4} S/cm, respectively. Therefore, the addition of conductive NiP leads to an

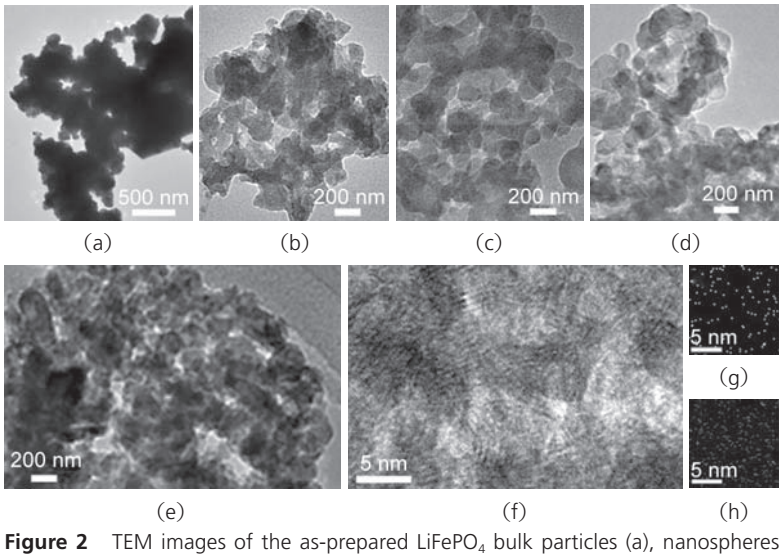

Figure 2 TEM images of the as-prepared $LiFePO_4$ bulk particles (a), nanospheres without NiP (b) and containing 0.35 wt% (c), 0.86 wt% (d), and 1.50 wt% (e) NiP. HRTEM image (f) of the middle sphere in (d), and the EDX mapping of Ni (g) and P (h)

increase in the electrical conductivity of $LiFePO_4$ by three to four orders of magnitude. The homogeneous distribution of amorphous NiP in the porous $LiFePO_4$ nanospheres contributes to the enhanced electrical conductivity.

2.2 Electrochemical measurements

Figure 3 shows the CVs of the electrodes made from the as-prepared $LiFePO_4$ bulk particles and $LiFePO_4$/NiP composite nanospheres in the first cycle. Similar voltammograms were also obtained for the following five cycles. Reversible peaks were observed for the electrodes composed of bulk particles and nanospheres, but the observed peak positions and currents were different. The results shown in Table 1 confirm that the addition of 0.86 wt%–1.50 wt% NiP is very effective in increasing the kinetics of reversible Li^+ insertion/extraction in the electrodes.

EIS has been proven to be a valuable and widely used technique to evaluate electrode kinetics [27, 28]. Therefore, the activation energies (E_a) of lithium extraction for the as-prepared $LiFePO_4$/NiP composite nanospheres were measured by EIS. Figure 4 shows the EIS of the as-prepared $LiFePO_4$/NiP composite nanospheres. The impedance curves for the samples have a similar profile with one semicircle with different radii in the high frequency region and a sloping line in the low frequency region. The equivalent circuit for the impedance spectra is shown in Fig. 4(f). After fitting the equivalent circuit, we can obtain the charge transfer impedance (R_{ct}). The apparent activation energies (E_a) of lithium-ion insertion/extraction for the samples can be calculated by the Arrhenius equation (Eq. 1),

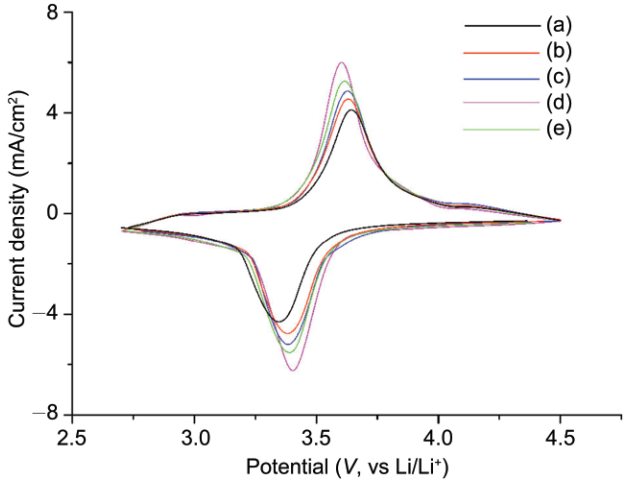

Figure 3 Cyclic voltammograms of the electrodes made from the as-prepared $LiFePO_4$ bulk particles (a), nanospheres without NiP (b) and containing 0.35 wt% (c), 0.86 wt% (d), and 1.50 wt% NiP (e) in the first cycle. The scan rate was 1 mV/s and the temperature 20 °C

Table 1 Summary of the cyclic voltammetry measurements

Electrode	Potential values (V)			Current densities (mA/cm^2)	
	E_R	E_O	E_O–E_R	I_R	I_O
$LiFePO_4$ bulk particles	3.343	3.643	0.300	4.36	4.07
Pure $LiFePO_4$ nanospheres	3.380	3.630	0.250	4.82	4.53
$LiFePO_4$/0.35 wt% NiP nanospheres	3.385	3.629	0.244	5.18	4.89
$LiFePO_4$/0.86 wt% NiP nanospheres	3.404	3.601	0.197	6.31	6.01
$LiFePO_4$/1.50 wt% NiP nanospheres	3.390	3.615	0.225	5.59	5.25

E_R: reduction potential; E_O: oxidation potential; I_R and I_O: the corresponding current densities.

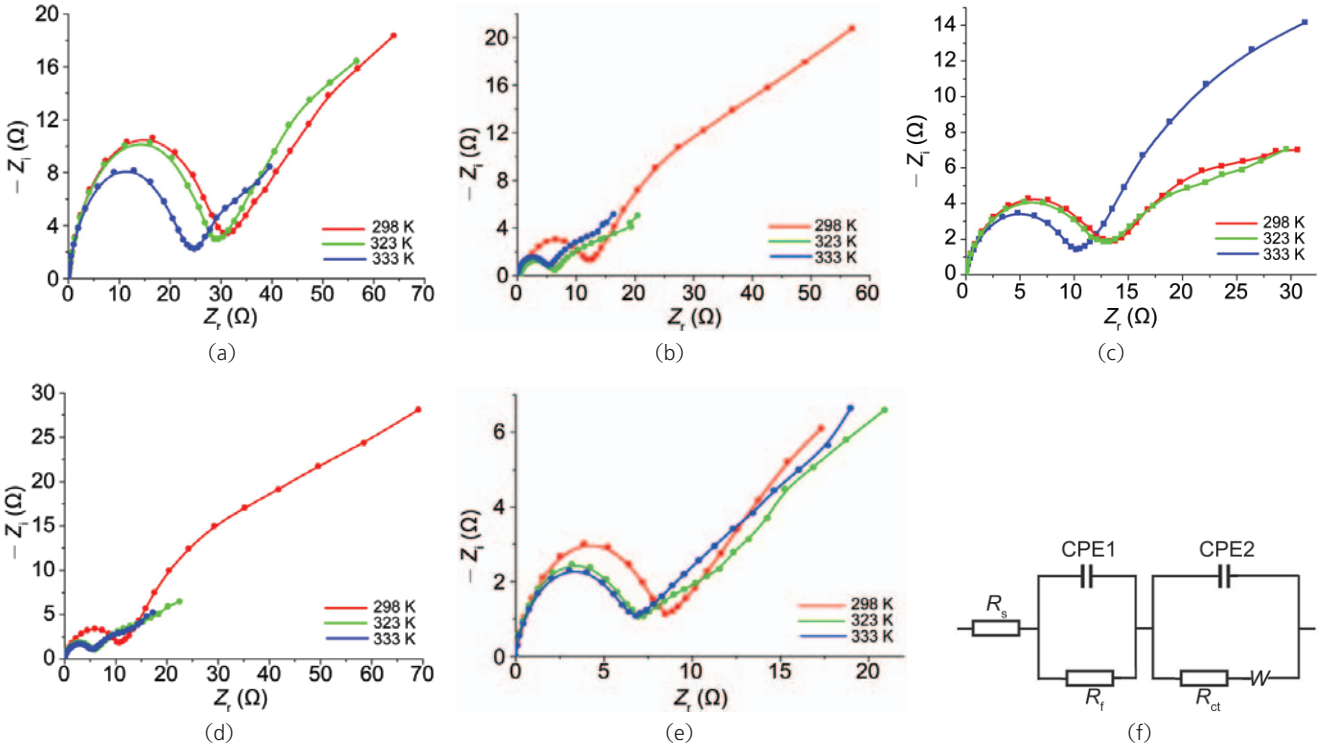

Figure 4 EIS of the as-prepared $LiFePO_4$/NiP composite nanospheres measured with a discharging voltage of 3.30 V and temperatures of 298, 323, and 333 K: $LiFePO_4$ bulk particles (a), nanospheres without NiP (b) and containing 0.35 wt% (c), 0.86 wt% (d), and 1.50 wt% NiP (e). The equivalent circuit for the impedance spectra of the samples is shown in (f)

$$\ln(T/R_{ct}) = -E_a/RT + \ln A' \quad (1)$$

where T is the absolute temperature, R_{ct} is the charge transfer impedance, E_a is the activation energy, R is the gas constant, and A' is a temperature-independent coefficient. The Arrhenius plots are shown in Fig. S-3 (in the ESM). The activation energies of the as-prepared $LiFePO_4$ bulk particles, nanospheres without NiP, and nanospheres containing 0.35 wt%, 0.86 wt%, and 1.5 wt% NiP are 24.5, 23.8, 22.5, 9.0, and 13.9 kJ/mol, respectively. It can be seen that $LiFePO_4$ nanospheres with the addition of 0.86 wt% NiP have lowest activation energy, indicating the fastest lithium insertion/extraction.

Figure 5 shows the charge-discharge curves of the electrodes made from various $LiFePO_4$ samples at a current density of 50 mA/g and 20 °C. Compared with the electrode composed of $LiFePO_4$ bulk particles, the electrodes made of nanospheres display lower charge plateaus and higher discharge plateaus, indicating their capability of high power output. The discharge capacities for the electrodes composed of the as-prepared $LiFePO_4$ bulk particles, nanospheres without NiP, and nanospheres containing 0.35 wt%, 0.86 wt%, and 1.5 wt% NiP are 125.9, 144.0, 158.4, 162.3, and 159.8 mAh/g, respectively. Therefore, the charge and discharge performance of $LiFePO_4$ electrode is significantly improved by the addition of NiP and the optimum content of NiP is 0.86 wt%.

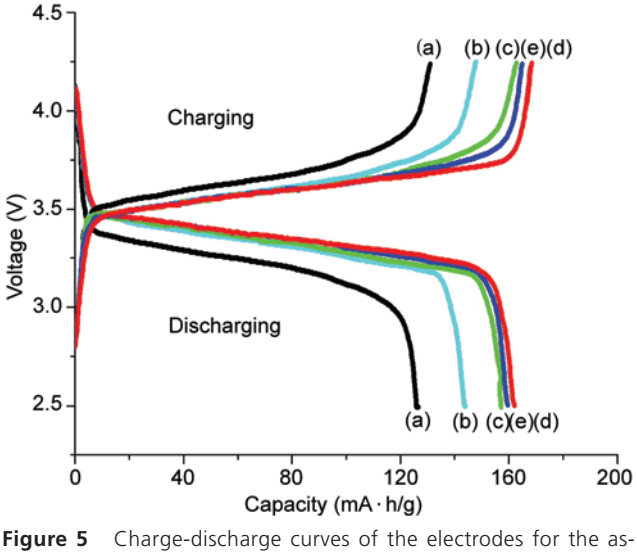

Figure 5 Charge-discharge curves of the electrodes for the as-prepared $LiFePO_4$ bulk particles (a), nanospheres without NiP (b) and containing 0.35 wt% (c), 0.86 wt% (d), and 1.50 wt% NiP (e) at a current density of 50 mA/g and temperature of 20 °C

Figure 6 shows the curves of discharge capacity versus cycle number for the electrodes made from different $LiFePO_4$ samples at a current density of 50 mA/g and 20 °C. After 50 cycles with 100% depth of charge and discharge, the electrodes of the as-prepared $LiFePO_4$ bulk particles (a), nanospheres without NiP (b), and nanospheres containing 0.35 wt% (c), 0.86 wt% (d), and 1.5 wt% NiP (e) are 119.1, 140.8, 155.9, 160.8, and 158.2 mAh/g, respectively. The rate of capacity decay in Fig. 6 displays the following order: (d) < (e) < (c) < (b) < (a), showing that the cycling capability of $LiFePO_4$ nanospheres can be improved by the addition of NiP.

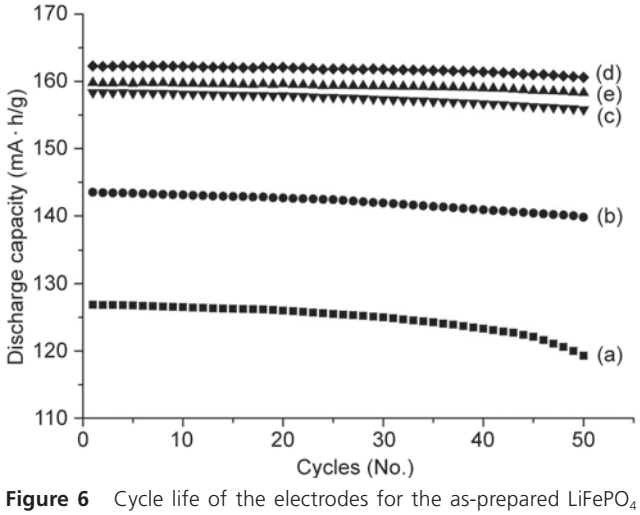

Figure 6 Cycle life of the electrodes for the as-prepared $LiFePO_4$ bulk particles (a), nanospheres without NiP (b) and containing 0.35 wt% (c), 0.86 wt% (d), and 1.50 wt% NiP (e) at a current density of 50 mA/g and temperature of 20 °C

The $LiFePO_4$/NiP composite electrodes display superior electrochemical properties to those of the $LiFePO_4$ electrode composed of bulk particles. This enhancement results from the increased electrical conductivity, larger specific surface areas, porous nanostructures with disorder, and low internal and charge-transfer resistance. Overall, the optimum NiP content in the $LiFePO_4$ nanospheres is around 0.86 wt%; this material has a low apparent activation energy of only 9.0 kJ/mol for lithium insertion/extraction. Furthermore, the as-prepared nanospheres have higher tapping density and better fluidity and dispersivity than the powders composed of irregular particles, which may be beneficial in the manufacture of high quality electrodes. Therefore, $LiFePO_4$/NiP composite nanospheres are promising candidates for use as the cathode materials in rechargeable lithium-ion batteries with high energy, high power, high safety, and long life, of the type which are needed for pure or hybrid electric vehicles.

3. Conclusions

The synthesis of $LiFePO_4$/NiP composite nanospheres with porous structures has been realized through a facile one-step spraying technique under mild conditions with low cost inorganic salts as precursors. It is found that by doping $LiFePO_4$ with 0.35 wt%–1.50 wt% amorphous NiP, the electrical conductivity of the composite nanospheres is dramatically improved by three or four orders of magnitude compared to bulk $LiFePO_4$. Cyclic voltammetry and galvanostatic results illustrated that both pure $LiFePO_4$ and $LiFePO_4$/NiP composite nanospheres exhibit superior electrochemical performance to that of bulk $LiFePO_4$. The optimum amount of NiP in the porous nanospheres is around 0.86 wt%. This study indicates that $LiFePO_4$/NiP composite nanospheres are promising cathode materials for use in rechargeable lithium-ion batteries with high capacity, high power, and long life.

Acknowledgments

This work was supported by the National Key Basic Research Program (2005CB623607), National Natrual Science Foundation of China (20703026) and Tianjin Basic & High-Tech Programs (07ZCGHHZ00700 and 08JCZDJC21300).

Electronic Supplementary Material: Supplementary material is available in the online version of this article at http://dx.doi.org/10.1007/s12274-008-8028-1 and is accessible free of charge.

References

[1] Tombler, T. W.; Zhou, C. W.; Alexseyev, L.; Kong, J.; Dai, H. J.; Lei, L.; Jayanthi, C. S.; Tang, M. J.; Wu, S. Y. Reversible electromechanical characteristics of carbon nanotubes under local-probe manipulation. *Nature* **2000**, *405*, 769–772.

[2] Law, M.; Greene, L. E.; Johnson, J. C.; Saykally, R.; Yang, P. D. Nanowire dye-sensitized solar cells. *Nat. Mater*. **2005**, *4*, 455–459.

[3] Wang, Z. L. Energy harvesting for self-powered nanosystems. *Nano Res.* **2008**, *1*, 1–8.

[4] Liu, J. F.; Chen, W.; Liu, X. W.; Zhou, K. B.; Li, Y. D. Au/$LaVO_4$ Nanocomposite: Preparation, characterization, and catalytic activity for CO oxidation. *Nano Res.* **2008**, *1*, 46–55.

[5] Padhi, A. K.; Nanjundaswamy, K. S.; Masquelier, C.; Okada, S.; Goodenough, J. B. Effect of structure on the Fe^{3+}/Fe^{2+} redox couple in iron phosphates. *J. Electrochem. Soc*. **1997**, *144*, 1609–1613.

[6] Tarascon, J. M.; Armand, M. Issues and challenges facing rechargeable lithium batteries. *Nature* **2001**, *414*, 359–367.

[7] Whittingham, M. S. Lithium batteries and cathode materials. *Chem. Rev*. **2004**, *104*, 4271–4301.

[8] Yamada, A.; Koizumi, H.; Nishimura, S. I.; Sonoyama, N.; Kanno, R.; Yonemura, M.; Nakamura, T.; Kobayashi, Y. Room-temperature miscibility gap in Li_xFePO_4. *Nat. Mater*. **2006**, *5*, 357–360.

[9] Whittingham, M. S. Materials challenges facing electrical energy storage. *MRS Bull*. **2008**, *33*, 411–419.

[10] Chen, Z. H.; Dahn, J. R. Reducing carbon in $LiFePO_4$/C composite electrodes to maximize specific energy, volumetric energy, and tap density. *J. Electrochem. Soc*. **2002**, *149*, A1184–A1189.

[11] Huang, H.; Yin, S. C.; Nazar, L. F. Approaching theoretical capacity of $LiFePO_4$ at room temperature at high rates. *Electrochem. Solid-State Lett*. **2001**, *4*, A170–A172.

[12] Takeuchi, T.; Tabuchi, M.; Nakashima, A.; Nakamura, T.; Miwa, Y.; Kageyama, H.; Tatsumi, K. Preparation of dense $LiFePO_4$/C composite positive electrodes using spark-plasma-sintering process. *J. Power Sources* **2005**, *146*, 575–579.

[13] Xie, H. M.; Wang, R. S.; Ying, J. R.; Zhang, L. Y.; Jalbout, A. F.; Yu, H. Y.; Yang, G. L.; Pan, X. M.; Su, Z. M. Optimized $LiFePO_4$–polyacene cathode material for lithium-ion batteries. *Adv. Mater*. **2006**, *18*, 2609–2613.

[14] Prosini, P. P.; Carewska, M.; Scaccia, S.; Wisniewski, P.; Pasquali, M. Long-term cyclability of nanostructured $LiFePO_4$. *Electrochim. Acta* **2003**, *48*, 4205–4211.

[15] Chung, S. Y.; Bloking, J. T.; Chiang, Y. M. Electronically conductive phospho-olivines as lithium storage electrodes. *Nat. Mater.* **2002**, *1*, 123–128.

[16] Herle, P. S.; Ellis, B.; Coombs, N.; Nazar, L. F. Nano-network electronic conduction in iron and nickel olivine phosphates. *Nat. Mater.* **2004**, *3*, 147–152.

[17] Nakamura, T.; Miwa, Y.; Tabuchi, M.; Yamada, Y. Structural and surface modifications of $LiFePO_4$ olivine particles and their electrochemical properties. *J. Electrochem. Soc.* **2006**, *153*, A1108–A1114.

[18] Gabrisch, H.; Wilcox, J. D.; Doeff, M. M. Carbon surface layers on a high-rate $LiFePO_4$. *Electrochem. Solid-State Lett*. **2006**, *9*, A360–A363.

[19] Lee, J.; Teja, A. S. Synthesis of $LiFePO_4$ micro and nanoparticles in supercritical water. *Mater. Lett*. **2006**, *60*, 2105–2109.

[20] Ng, S. H.; Wang, J. Z.; Wexler, D.; Konstantinov, K.; Guo, Z. P.; Liu, H. K. Highly reversible lithium storage in spheroidal carbon-coated silicon nanocomposites as anodes for lithium-ion batteries. *Angew. Chem. Int. Ed.* **2006**, *45*, 6896–6899.

[21] Cheng, F. Y.; Zhang, S. Y.; Tao, Z. T.; Liang, J.; Chen, J. $LiFePO_4$/NiP composite microspheres as the cathode materials of rechargeable lithium-ion batteries. In *IMLB 2008 Abstract 395*; The 14th Int. Meeting on Lithium Batteries Tianjin, China, June 22–28, 2008.

[22] Chen, J.; Xu, L. N.; Li, W. Y.; Gou, X. L. Alpha-Fe_2O_3 nanotubes in gas sensor and lithium-ion battery applications. *Adv. Mater*. **2005**, *17*, 582–286.

[23] Yamada, A.; Chung, S. C.; Hinokuma, K. Optimized $LiFePO_4$ for lithium battery cathodes. *J. Electrochem. Soc.* **2001**, *148*, A224–A229.

[24] Izumi, F.; Ikeda, T. A Rietveld analysis program RIETAN-98 and its applications to zeolites. *Mater. Sci. Forum* **2000**, *321–324*, 198–203.

[25] Li, W. Y.; Li, C. S.; Zhou, C. Y.; Ma, H.; Chen, J. Metallic magnesium nano/mesoscale structures: Their shape-controlled preparation and Mg/Air battery applications. *Angew. Chem. Int. Ed.* **2006**, *45*, 6009–6012.

[26] Ma, H.; Cheng, F. Y.; Chen, J.; Zhao, J. Z.; Li, C. S.; Tao, Z. L.; Liang, J. Nest-like silicon nanospheres for high-capacity lithium storage. *Adv. Mater.* **2007**, *19*, 4067–4070.

[27] Ma, H.; Zhang, S. Y.; Ji, W. Q.; Tao, Z. L.; Chen, J. Alpha-CuV_2O_6 nanowires: Hydrothermal synthesis and primary lithium battery application. *J. Am. Chem. Soc.* **2008**, *130*, 5361–5367.

[28] Ma, H.; Li, C. S.; Su, Y.; Chen, J. Studies on the vapour-transport synthesis and electrochemical properties of zinc micro-, meso- and nanoscale structures. *J. Mater. Chem*. **2007**, *17*, 684–691.